Cis−Trans Photoisomerization of the 1,6-Diphenyl-1,3,5-hexatrienes in the Triplet State. The Quantum Chain Mechanism and the Structure of the Triplet State†

Jack Saltiel,* Shujun Wang, Dong-Hoon Ko, and David A. Gormin

Department of Chemistry, The Florida State University, Tallahassee, Florida 32306-4390

Received: September 9, 1997; In Final Form: November 5, 1997

Fluorenone sensitization in solution interconverts *all-trans*-1,6-diphenyl-1,3,5-hexatriene (*ttt*-DPH) with its trans,cis,trans, cis,trans,trans, and cis,cis,trans (trace) isomers, *tct*-, *ctt*-, and *cct*-DPH, respectively. Photoisomerization quantum yields are reported for the three major isomers in degassed and air-saturated benzene. In degassed solutions the quantum yields are strongly concentration dependent due to quantum chain processes. The presence of air eliminates the quantum chain processes, as all DPH triplets are deactivated by oxygen. Triplet−triplet absorption spectra observed in the microsecond time scale starting from these three DPH isomers are identical. The concentration dependence of the DPH triplet lifetime is consistent with the concentration dependence of the isomerization quantum yields. The results indicate that in benzene DPH triplets exist as an equilibrium mixture of ttt, tct, and ctt isomers whose composition at 20 °C, 94% ttt, 5% tct, and 1% ctt is revealed by isomerization quantum yields in the presence of air. Photoisomerization quantum yields in the presence of air show that the isomeric triplets are fully equilibrated within less than 100 ns.

Introduction

all-trans-1,6-Diphenyl-1,3,5-hexatriene (*ttt*-DPH) is the shortest α,ω-diphenylpolyene whose spectroscopy mimics that of the longer polyenes.[1−3] It is the first member of the series whose lowest excited singlet state is the forbidden doubly excited 2^1A_g state that plays a prominent role in the Orlandi and Siebrand mechanism for stilbene photoisomerization.[4] In *ttt*-DPH the initially formed 1^1B_u state is sufficiently close in energy to the 2^1A_g state that the two states mix via vibronic coupling to give mixed states that exist in thermal equilibrium.[5] In view of the $1^1B_u \rightleftharpoons 2^1A_g$ equilibration, both states are viable intermediates for photoisomerization.[6] Until recently,[7,8] the focus has been on the 2^1A_g state[9−11] as the key intermediate based on Birks' extension of the Orlandi and Siebrand photoisomerization model for the stilbenes to α,ω-diphenylpolyenes.[12] The assumption inherent in this mechanism, that fluorescence and photoisomerization channels are complementary processes originating in the S_1 state of the α,ω-diphenylpolyenes, was not borne out by the small photoisomerization quantum yields obtained on direct excitation of the DPH isomers,[7] nor did our work reveal any special relationship between the relative order of the 1^1B_u and the 2^1A_g states and photoisomerization efficiency.[8] The latter result is, or course, consistent with the finding that equilibration between these two states is complete within at most 10 ps.[6]

At the outset of our work, the conclusion that triplet states are not involved in the photoisomerization of *ttt*-DPH seemed secure. Triplet−triplet absorption either was not detected following direct *ttt*-DPH excitation[13,14] or was very small when detected, $\phi_{is} = 0.024-0.029$ in benzene, cyclohexane, or ethanol at ambient temperature.[15−17] Furthermore, ^{3}*ttt*-DPH* formed by energy transfer from suitable triplet energy donors was reported not to photoisomerize.[16] Since intersystem crossing quantum yields are not small when compared with the overall photoisomerization quantum yields under direct excitation conditions,[7] a reexamination of the behavior of DPH triplets seemed desirable.

Experimental Section

Materials. *all-trans*-1,6-Diphenyl-1,3,5-hexatriene (Aldrich, 98%) was chromatographed on silica gel with benzene/*n*-hexane (10:90, v/v) as eluent and then recrystallized twice from *n*-hexane to 99.99% (HPLC) purity. *ctt*- and *tct*-DPH, prepared photochemically from this material, were purified by gravity column chromatography and HPLC as previously described.[20] Benzophenone (Aldrich, 99%) was recrystallized twice from *n*-hexane and sublimed under vacuum (mp 48.0 °C, 99.98% purity, GLC). Fluorenone (Aldrich, 98%) was chromatographed on alumina with benzene as eluent and recrystallized twice on 95% ethanol (99.98% purity, GLC). *trans*-Stilbene (Aldrich, 96%) was recrystallized from ethanol, chromatographed from alumina with *n*-hexane as eluent and sublimed under reduced pressure (99.99% purity, GLC). Anthracene (Mallinckrodt, 90−95%) was recrystallized from ethanol and sublimed under vacuum (no impurity detected by HPLC). Anthraquinone and benzanthrone were as previously described.[21] Methylcyclohexane (MCH) (Eastman Kodak) was stirred over several portions of fuming sulfuric acid and then sulfuric acid, washed with aqueous sodium bicarbonate followed by distilled water, dried over magnesium sulfate, and fractionally distilled. Middle fractions collected from the distillation were employed that exceeded the UV transparency of Baker Photrex MCH. Acetonitrile and *n*-hexane (Fisher, Optima) were used as received. Metts benzene,[22] purified by Ms. C. Lau, was used initially for photochemical experiments; benzene (Fisher, Spectranalyzed), passed through alumina, gave identical results. Alumina (Woelm), flushed with 1 L of 6 N nitric acid, then with 2 L of deionized water, and finally with 700 mL of methanol (Fisher, distilled), was dried in an oven for 4 days at 130 °C.

Absorption Spectra. Absorption spectra were measured with the use of a Perkin-Elmer Lambda-5 spectrophotometer interfaced with a Dell Corp. 12-MHz 80286/87 microcomputer.

† J.S. dedicates this paper to his teacher, George S. Hammond, whose illuminating and inspiring ways made this issue possible.

S1089-5639(97)02941-1 CCC: $15.00
Published on Web 02/12/1998

Transient Absorption Measurements. The third harmonic, 355 nm, 7−9 ns pulse width, from an Nd:YAG laser (Quanta Ray DCR 2A, Spectra Physics) was used to pump a dye laser (Quanta Ray PDL 2, Spectra Physics) system. Coumarin 2 (Fisher) in methanol was employed to generate 445−475 nm laser pulses. A monochromator (Jarrell Ash), was employed to select $\lambda_{exc} = 450$ nm for transient excitation. Pulse energy was monitored with an energy power meter (RJP-735, Laser Precision Corp.) and adjusted to 60 μJ/pulse to minimize dye/DPH decomposition/photoisomerization, and triplet−triplet annihilation decay events and to ensure linear DPH absorption. Triplet transient decay was probed with a xenon lamp (Oriel, 75-W) at 90° to the excitation pulse. A UV cutoff filter (L-390) was used to reduce exposure of the sample to probe light. Light transmitted through the sample was passed through a monochromator (Jerrell Ash) and was detected by a Hamamatsu R 928 photomultiplier tube with the use of a digital oscilloscope (LeCroy model 9410 dual-channel, 150 MHz) where it was summed and averaged and then transferred to an IBM PC 80386 computer.

Transient absorption measurements were made at ambient temperature, 20−22 °C. Homemade 1 cm square Pyrex cells were employed for lifetime measurements. Solutions were placed in cyclindrical ampules connected to the cells by side arms and were degassed using at least six freeze−pump−thaw cycles to $<2.5 \times 10^{-5}$ Torr. The ampules were flame-sealed at a constriction. To acquire data for each transient absorption spectrum the sample was flowed through a 1 cm path length fused silica cell at a sufficiently high rate to replace the volume of the solution that was exposed to the excitation pulses impinging on the sample at a rate of 10 pulses/s. Sample solutions contained in a reservoir were argon-bubbled via a fritted glass disk for at least 4 h prior to the measurements and throughout each experiment. A prebubbler containing the identical solution was employed to avoid solvent loss. To improve signal-to-noise ratio, each point of each difference spectrum is the average of the result of at least 100 excitation laser pulses. Following the measurement of each spectrum the degree of DPH photoisomerization was determined by HPLC (see below).

Irradiation Procedure. Solutions, 3.0 mL, were pipetted into Pyrex ampules, 13 mm o.d., fitted with 10/30 standard-taper joints and grease traps. Degassing was achieved using 5−6 freeze−pump−thaw cycles to $<1.5 \times 10^{-5}$ Torr and the ampules were flame-sealed at a constriction. Sample preparation and degassing were performed under nearly complete darkness and degassed ampules, wrapped in aluminum foil, were stored in the freezer until used. Air-saturated solutions were stoppered loosely with Teflon-covered stoppers. A miniature merry-go-round whose rotation was controlled by a GT 21 motor (Gerald K. Heller Co.) was immersed in a thermostated water bath. Incident light was from an Osram HBO 200 W super high-pressure mercury lamp or from an Osram 150 W/L xenon lamp using a Bausch & Lomb SP-200 lamp housing and a Schoeffel LPS 251 power supply. Exciting wavelengths (415−450 nm) were selected with the use of a high-intensity Bausch and Lomb monochromator. Fluorenone-sensitized photoisomerization of *trans*-stilbene in benzene ($\phi_{tc} = 0.47$[23,24]) was employed for actinometry. Concentration of DPH and of the sensitizer were sufficiently high to ensure total absorption of incident light. Conversions were corrected for back reaction.[25−27] Crystallization of *ttt*-DPH occurs in ampules stored in the freezer and it was necessary to ensure solution uniformity prior to irradiation.

TABLE 1: Attainment of Photostationary States for the Fluorenone-Sensitized Photoisomerization of DPH, $\lambda_{exc} = 425$ nm, Degassed Bz, MCH

10^3[*ttt*-DPH], M	*t*, min	f_{ctt}	f_{tct}	f_{cct}	f_{ttt}[a]
0.412[b]	26	0.0313	0.0901	0.00217	0.876
	32	0.0333	0.0938	0.00239	0.871
	37	0.0353	0.0964	0.00260	0.866
0.824[b]	45	0.0351	0.0990	0.00255	0.863
	52	0.0360	0.0998	0.00273	0.861
1.07[c]	30	0.0306	0.0811		0.888
	50	0.0363	0.0954		0.868
	70	0.0361	0.0939		0.870
	90	0.0371	0.0967		0.866
	110	0.0377	0.0980		0.864
	210	0.0353	0.0981		0.862
4.12[b]	52	0.0297	0.0846	0.00217	0.884
	65	0.0314	0.0879	0.00236	0.878
	72	0.0322	0.0903	0.00252	0.875

[a] $f_{ttt} = 1 - \Sigma f_p$, where p designates cis products. [b] Benzene, 25 °C. [c] Methylcyclohexane, 20 °C; direct HPLC analysis for *ttt*-DPH gave 97 ± 3% mass balance; in a separate experiment, analysis with $\lambda_{mon} = 270$ nm revealed no additional products.

Analytical Procedures. Actinometer solutions were analyzed by GLC on a Varian 3300 instrument operated over a programmed temperature range (160 → 180 °C, 1 °C/min) using a J & W Scientific DX-4 capillary column. Prior to analysis, actinometer solutions were concentrated to about one-third the original volume, using a gentle stream of N_2. GLC analysis of DPH products was unsuccessful due to product instability. DPH analysis was achieved by HPLC using anthracene, A, as an internal standard. Except for MCH, the considerable influence of different solvents on retention times, peak shapes, and areas of the DPH isomers was avoided by replacing the solvents (rotary evaporation under reduced pressure) with a standard solution of A in *n*-hexane. The purity of *n*-hexane as storing, replacing, or eluting solvent is critical. For instance, substantial loss of cis isomers (especially *tct*-DPH) was observed when HPLC grade *n*-hexane was employed. No such losses were experienced with Fisher, Optima grade, *n*-hexane. Sample preparations and analyses were performed in nearly complete darkness. All samples were analyzed at least in duplicate, on a normal-phase SI column (Beckman Ultrasphere, analytical 4.6 × 250 mm) immediately following irradiation and solvent replacement (except for MCH). Samples reanalyzed after standing for a week in the dark showed no change in isomer distribution. No products other than the cis isomers were detected even after prolonged irradiation (photostationary state solutions were monitored at both 270 and 350 nm). Standard solutions were employed to establish linear instrumental range and relative response factors, 1.00:1.00:0.90 for *ttt*-, *tct*-, and *ctt*-DPH, respectively (see ref 28 for details). Product absorptivities at 350 nm were identical to those published earlier 43 200 and 51 530 M^{-1} cm^{-1} for *ctt*- and *tct*-DPH, respectively.[29] Accordingly, the published value[29] of 37 000 M^{-1} cm^{-1} was employed for *cct*-DPH.

Results

Photochemical Observations. Unless otherwise indicated, fractional compositions of the DPH isomers were measured by employing $\lambda_{mon} = 350$ nm in the HPLC analyses. The time required under our irradiation conditions for degassed benzene and methylcyclohexane solutions of *ttt*-DPH to attain photostationary compositions was determined for the fluorenone-sensitized photoisomerization, Table 1. Photostationary states for these two solvents in the presence of air are shown in Table

TABLE 2: Photostationary States for the Fluorenone-Sensitized Photoisomerization of DPH in Air-Saturated Bz, MCH[a]

10^3[DPH], M	f_{ctt}	f_{tct}	f_{cct}[b]	f_{ttt}	f_{ctt}/f_{tct}
0.274[c]	0.0102	0.0412		0.949	0.248
0.429[d]	0.0108	0.0398	0.00042	0.921[e]	0.270
0.417	0.0071	0.0302	0.00014	0.963	0.236
0.487	0.0070	0.0307	0.00013	0.962	0.227
0.626	0.0080	0.0335	0.00017	0.958	0.240
0.834	0.0075	0.0323	0.00015	0.960	0.233
1.298	0.0072	0.0316	0.00014	0.961	0.228

[a] Unless otherwise indicated, *tct*-DPH solutions were irradiated in Bz for 1920 min at 450 nm, 23 °C, and f_{ttt} obtained by difference as in Table 1. [b] *cct*-DPH appeared as a small shoulder at the tail of the *ctt*-DPH peak. It was quantitated by cutting and weighing the HPLC peaks. [c] *ttt*-DPH solution in MCH was irradiated for 960 min at 435 nm, 20 °C. [d] *ttt*-DPH solution in MCH irradiated for 1920 min at 450 nm, 22 °C. [e] Measured directly by HPLC.

TABLE 3: Photostationary States for the Fluorenone-Sensitized Photoisomerization of DPH in Degassed Acetonitrile, 425 nm, 20 °C[a]

10^3[*ttt*-DPH], M	f_{ctt}	f_{tct}	f_{ttt}
0.274	0.013	0.084	0.903
0.548	0.011	0.079	0.910
0.821	0.012	0.072	0.917
1.10	0.012	0.077	0.912
1.37	0.011	0.076	0.913

[a] All samples irradiated for 90 min; $f_{ttt} = 1 - \sum f_p$.

TABLE 4: Quantum Yields for the Fluorenone-Sensitized Photoisomerization of *ttt*-DPH in Benzene, 20 °C[a]

10^3[*ttt*-DPH], M	ϕ_{ctt}	ϕ_{tct}	ϕ_{ctt}/ϕ_{tct}
Degassed, 430 nm			
0.274	0.038	0.164	0.234
0.370	0.052	0.215	0.240
0.506	0.064	0.276	0.233
0.548	0.072	0.302	0.233
0.675	0.084	0.359	0.235
0.821	0.105	0.455	0.231
1.00	0.128	0.556	0.230
1.01	0.110	0.475	0.233
1.10	0.131	0.573	0.229
1.37	0.156	0.685	0.228
2.03	0.187	0.818	0.228
1.14[b]	0.090	0.38	0.239
1.14[c]	0.019	0.077	0.248
Air-Saturated, 450 nm			
0.428	0.0033_4	0.0147	0.227
0.510	0.0037_9	0.0164	0.231
0.612	0.0042_2	0.0183	0.230
0.816	0.0050_0	0.0218	0.229
1.22	0.0060_2	0.0264	0.228

[a] Estimated error in quantum yields ±4%. [b] Anthraquinone sensitizer. [c] Benzanthrone sensitizer.

2. Photostationary states in degassed acetonitrile as a function of initial [*ttt*-DPH] are shown in Table 3. Quantum yields for the fluorenone-sensitized photoisomerization of *ttt*-DPH in benzene and in methylcyclohexane as a function of [*ttt*-DPH] are shown in Tables 4 and 5, respectively, under degassed and air-saturated conditions. Quantum yields for degassed solutions of *ttt*-DPH in carbon tetrachloride and in acetonitrile are shown in Table 6. Photoisomerization quantum yields for *ctt*-DPH and *tct*-DPH in degassed and air-saturated benzene are shown in Tables 7 and 8, respectively. Starting from *ttt*-DPH total conversions to the other isomers were ≤3.0% and ≤0.6% for degassed and air-saturated solutions, respectively. The corresponding conversions starting from *tct*- and from *ctt*-DPH were ≤22% and ≤8%.

TABLE 5: Quantum Yields for the Fluorenone-Sensitized Photoisomerization of *ttt*-DPH in Methylcyclohexane, 20 °C, 420 nm[a]

10^3[*ttt*-DPH],[b] M	ϕ_{ctt}	ϕ_{tct}	ϕ_{ctt}/ϕ_{tct}
Degassed			
0.532 (0.513)	0.041	0.168	0.246
0.798 (0.764)	0.067	0.280	0.239
1.54 (1.48)	0.092	0.371	0.247
1.84 (1.76)	0.111	0.468	0.237
Air-Saturated[c]			
0.532	0.0048	0.0183	0.263
0.798	0.0061	0.0239	0.257
1.54	0.0088	0.0338	0.260
1.84	0.0103	0.0401	0.257

[a] Estimated quantum yield uncertainties ± 4%. [b] Values in parentheses are effective [*ttt*-DPH] = $[1 - (f_{ctt} + f_{tct})/2][ttt\text{-DPH}]_0$. [c] Total isomer conversions were <0.8%. A duplicate experiment carried out to ~1.8% total conversions resulted in quantum yields in excellent agreement with those given here, but back reaction corrections were large.

TABLE 6: Quantum Yields for the Fluorenone-Sensitized Photoisomerization of *ttt*-DPH in CCl_4 and CH_3CN[a]

10^3[*ttt*-DPH], M	ϕ_{ctt}	ϕ_{tct}	ϕ_{ctt}/ϕ_{tct}
CCl_4, Degassed, 21 °C, 415 nm[b]			
0.411 (4.02)	0.064	0.132	0.485
0.822 (8.07)	0.107	0.201	0.532
4.11 (4.04)	0.357	0.730	0.489
8.22 (8.10)	0.586	1.11	0.528
CH_3CN, Degassed, 20 °C, 430 nm[c]			
0.339 (0.337)	0.019	0.125	0.154
0.407 (0.404)	0.025	0.136	0.181
0.509 (0.506)	0.028	0.154	0.180
0.679 (0.675)	0.039	0.206	0.188
1.02 (1.01)	0.050	0.289	0.174

[a] Estimated quantum yield uncertainties ± 4%; values in parentheses are effective concentrations. [b]Conversion range, 2.9−4.6%. [c]Conversion range, 1.0−1.4%.

TABLE 7: Quantum Yields for the Fluorenone-Sensitized Photoisomerization of *ctt*-DPH in Benzene, 20 °C, 450 nm[a]

10^3[*ctt*-DPH],[b] M	ϕ_{tct}	ϕ_{ttt}	$\phi_{tct/\phi ttt}$
Degassed			
0.387 (0.347)	0.337	4.99	0.068
0.451 (0.402)	0.407	6.39	0.064
0.580 (0.523)	0.435	7.24	0.060
0.773 (0.700)	0.528	9.24	0.057
1.20 (1.10)	0.750	13.6	0.055
Air-Saturated[c]			
0.387 (0.372)	0.0131	0.288	0.046
0.451 (0.434)	0.0186	0.342	0.054
0.580 (0.560)	0.0183	0.381	0.048
0.773 (0.750)	0.0221	0.451	0.049
1.20 (1.18)	0.0282	0.540	0.052

[a] Estimated quantum yield uncertainties ±4%. [b] Values in parentheses are effective concentrations calculated from $[1 - (f_{ttt} + f_{tct})/2][ctt\text{-DPH}]_0$. [c] Lightly stoppered ampules.

Transient Measurements. The [*ttt*-DPH] dependencies of the triplet lifetimes of DPH in acetonitrile, benzene, and methylcyclohexane are shown in Table 9. Triplet−triplet absorption spectra obtained starting with pure *ttt*-DPH, *tct*-DPH and *ctt*-DPH solutions, ~1.0×10^{-3} M in benzene are shown in Figure 1. The initial isomeric purity of DPH samples was 100.0% for *ttt*-DPH and >99.5% for *ctt*- and *tct*-DPH. The final compositions, determined by HPLC analysis following the

TABLE 8: Quantum Yields for the Fluorenone-Sensitized Photoisomerization of *tct*-DPH in Benzene, 20 °C, 450 nm[a]

10^3[*tct*-DPH],[b] M	ϕ_{ctt}	ϕ_{ttt}	ϕ_{ctt}/ϕ_{ttt}
	Degassed		
0.417 (0.370)	0.082	6.37	0.0128
0.487 (0.429)	0.096	7.99	0.0121
0.626 (0.555)	0.113	9.68	0.0117
0.834 (0.734)	0.145	13.9	0.0105
1.30 (1.17)	0.176	17.4	0.0101
	Air-Saturated[c]		
0.417 (0.397)	0.00338	0.338	0.0115
0.487 (0.464)	0.00386	0.373	0.0103
0.626 (0.599)	0.00432	0.432	0.0100
0.834 (0.804)	0.00509	0.487	0.0104
1.30 (1.26)	0.00640	0.558	0.0100

[a] Estimated quantum yield uncertainties ±4%. [b] Values in parentheses are effective concentrations calculated from $[1 - (f_{ttt} + f_{ctt})/2][tct\text{-DPH}]_0$. [c] Lightly stoppered ampules.

TABLE 9: DPH Triplet Lifetimes, Degassed 20−22 °C

	τ,[a] μs		
10^3[*ttt*-DPH], M	CH_3CN	Bz	MCH
0.100	64.5	58.8	36.7
0.500	62.5	53.5	35.1
1.00	59.2	48.1	30.6
1.50	56.5	45.2	28.4
2.00	54.1	42.0	24.9

[a] Standard deviations of the first-order decay plots were less than ±1% of the observed lifetimes.

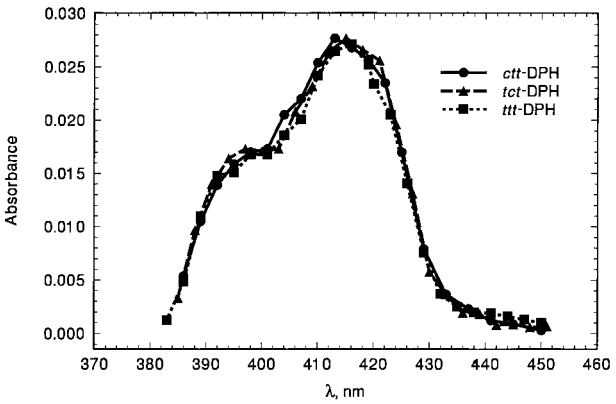

Figure 1. Transient triplet−triplet absorption spectra of benzene solutions of *ttt*-, *tct*-, and *ctt*-DPH, ■, ▲, and ●, respectively.

transient absorption measurements, were 0.15% ctt, 0.66% tct, and 99.2% ttt for the *ttt*-DPH sample, 0.30% ctt, 87.7% tct, and 12.0% ttt for the *tct*-DPH sample, and 88.3% ctt, 0.80% tct, and 10.9% ttt for the *ctt*-DPH sample. The points in the figure are absorbances 21 μs following the laser pulse (60 μJ). The lifetimes of the triplet transient for $[ctt\text{-DPH}] = 1.02 \times 10^{-3}$ M and $[tct\text{-DPH}] = 0.97 \times 10^{-3}$ M were 47.1 ± 0.5 and 48.9 ± 0.5 μs, respectively.

Discussion

Evidence supporting the conclusion[16,17] that the triplet state derived from *ttt*-DPH retains the all-trans planar geometry is as follows: (i) its long triplet lifetime in solution, in the microsecond time scale,[16,17,30] is consistent with a relatively large T_1-S_0 energy gap for the relaxed triplet state, (ii) the shape of its $T_n \leftarrow T_1$ absorption spectrum is not affected significantly on changing the medium from fluid solution at ambient temperature[15−17] to a rigid glass at 77 K,[16,31] (iii) its quenching by oxygen gives efficient formation of $O_2(^1\Delta_g)$,[32,33] and (iv) ^{3}DPH* formation via triplet excitation transfer gives no trans → cis photoisomerization.[16]

Contrary to (iv) above, the observations in Tables 1 and 2 under degassed conditions reveal that fluorenone sensitization yields photostationary states which, while rich in *ttt*-DPH, contain significant amounts of *tct*- and *ctt*-DPH and a trace of *cct*-DPH. In view of the strong DPH concentration dependencies of photoisomerization quantum yields (Tables 4−8), the photostationary states are relatively insensitive to initial DPH concentration. Strong enhancements of photoisomerization quantum yields in all directions with increasing concentration of the starting DPH isomer are consistent with quantum chain processes.[34−40] The decrease in the DPH triplet lifetime from the microsecond to the nanosecond[16,17] time scale in the presence of air eliminates quantum chain contributions to the photoisomerization and accounts for the large attenuation in photoisomerization quantum yields in air-saturated solutions.

The simplest mechanism that explains all the observations is shown below

$$^1F \xrightarrow{h\nu} {}^1F^* \xrightarrow{\phi_{is}} {}^3F^* \quad (1)$$

$$^3F^* + {}^1ttt \xrightarrow{k^F_{qttt}} {}^1F + {}^3eet^* \quad (2)$$

$$^3F^* + {}^1tct \xrightarrow{k^F_{qtct}} {}^1F + {}^3eet^* \quad (3)$$

$$^3F^* + {}^1ctt \xrightarrow{k^F_{qctt}} {}^1F + {}^3eet^* \quad (4)$$

$$^3F^* + {}^3O_2 \xrightarrow{k^F_{qox}} {}^1F + {}^1O_2^* \quad (5)$$

$$^3eet^* \xrightarrow{k_d} \alpha\,{}^1ctt + \beta\,{}^1tct + (1-\alpha-\beta)\,{}^1ttt \quad (6)$$

$$^3eet^* + {}^1ttt \xrightarrow{k_{ttt}} \gamma\,{}^1ctt + \delta\,{}^1tct + (\gamma+\delta)\,{}^3eet^* + 2(1-\gamma-\delta)\,{}^1ttt \quad (7)$$

$$^3eet^* + {}^1tct \xrightarrow{k_{tct}} \gamma'\,{}^1ctt + \delta'\,{}^1ttt + (\gamma'+\delta')\,{}^3eet^* + 2(1-\gamma'-\delta')\,{}^1tct \quad (8)$$

$$^3eet^* + {}^1ctt \xrightarrow{k_{ctt}} \gamma''\,{}^1tct + \delta''\,{}^1ttt + (\gamma''+\delta'')\,{}^3eet^* + 2(1-\gamma''-\delta'')\,{}^1ctt \quad (9)$$

$$^3eet^* + {}^3O_2 \xrightarrow{k_{qox}} \epsilon\,{}^1ctt + \zeta\,{}^1tct + (1-\epsilon-\zeta)\,{}^1ttt + {}^1O_2^* \quad (10)$$

where ϕ_{is} is the intersystem crossing yield of fluorenone and ^{3}eet* is an equilibrium mixture of planar DPH triplets:

$$^3eet^* \equiv {}^3ctt^* \overset{K_{10}}{\rightleftharpoons} {}^3ttt^* \overset{K_{03}}{\rightleftharpoons} {}^3tct^* \rightleftharpoons {}^3cct^* \quad (11)$$

Analogous steps involving *cct*-DPH are omitted because it forms in only trace amounts. An all-trans planar geometry for the DPH triplet is excluded by the results because ^{3}*ttt*-DPH* cannot serve as a chain carrier for photoisomerization in ttt → ctt, ttt → tct and ttt → cct directions. An equilibrium mixture of the all-trans triplet with nearly planar triplets containing cis double bonds provides the required chain carriers and is consistent with observation (i)−(iii) above.

Observations in Air-Saturated Solutions. The relationship between the efficiency and the products of the quenching of olefin triplets by oxygen with the geometry and the lifetime of olefin triplets is well established.[40−42] The prototypical short-

lived 62 ns[43] twisted triplet of stilbene is quenched by molecular oxygen by a spin-exchange mechanism with a rate constant close to $(3/9)k_{diff}$.[41] Quenching predominantly at a twisted geometry leaves the partitioning trans/cis ratio of the stilbene triplet unperturbed,[40−42] and is reflected in a small $O_2(^1\Delta_g)$ yield, 0.13−0.18.[44,45] On the other hand, longer-lived (μs−ms) planar olefin triplets undergo oxygen quenching by excitation transfer with rate constants closer to $(1/9)k_{diff}$,[42,46,47] the olefin product mirrors the geometry of the quenched triplet, and $O_2(^1\Delta_g)$ forms with nearly unit efficiency.[42] *ttt*-DPH falls cleanly into the latter category.[16,17] In view of our photoisomerization results, we have modified the earlier assignment of the all-trans geometry to the DPH triplet[16,17] by including small fractional contributions of triplets with cis double bonds in an equilibrium distribution dominated by the all-trans triplet.

If triplet equilibration is rapid relative to the triplet decay rate of DPH in air-saturated solutions, 1.0×10^7 s^{-1},[16,17] the O_2 quenching events summarized in eq 10 should provide a snapshot of the DPH triplet composition. Application of the steady state approximation on all excited species, based on the assumption of rapid equilibration, leads to the prediction that photostationary isomer ratios in the presence of air should be independent of the initial DPH concentration

$$\frac{[\mathrm{ttt}]_s}{[\mathrm{ctt}]_s} = \left(\frac{k^F_{qctt}}{k^F_{qttt}}\right)\left(\frac{1-\epsilon-\zeta}{\epsilon}\right) \tag{12}$$

$$\frac{[\mathrm{ctt}]_s}{[\mathrm{tct}]_s} = \left(\frac{k^F_{qtct}}{k^F_{qctt}}\right)\left(\frac{\epsilon}{\zeta}\right) \tag{13}$$

This condition, tested in Bz solutions (Table 2), is adhered to exactly. Photostationary fractions strongly favor the all-trans isomer, $f_{ttt} = 0.961 \pm 0.002$, independent of [DPH], although the starting isomer was *tct*-DPH. The mechanism requires that the same triplet distribution be obtained starting from any of the DPH isomers. Loss of memory of initial DPH geometry is reflected in quantum yields to each specific isomer that are nearly independent of the identity of the starting isomer.

$$\frac{\phi_{is}}{\phi_{ctt}} = \frac{1}{\epsilon}\left(1 + \frac{k^F_{qox}[O_2]}{k^F_{qttt}[\mathrm{ttt}]}\right) \simeq \frac{1}{\epsilon}\left(1 + \frac{k^F_{qox}[O_2]}{k^F_{qtct}[\mathrm{tct}]}\right) \tag{14}$$

$$\frac{\phi_{is}}{\phi_{tct}} = \frac{1}{\zeta}\left(1 + \frac{k^F_{qox}[O_2]}{k^F_{qttt}[\mathrm{ttt}]}\right) \simeq \frac{1}{\zeta}\left(1 + \frac{k^F_{qox}[O_2]}{k^F_{qctt}[\mathrm{ctt}]}\right) \tag{15}$$

$$\frac{\phi_{is}}{\phi_{ttt}} = \frac{1}{1-\epsilon-\zeta}\left(1 + \frac{k^F_{qox}[O_2]}{k^F_{qctt}[\mathrm{ctt}]}\right) \simeq \frac{1}{1-\epsilon-\zeta}\left(1 + \frac{k^F_{qox}[O_2]}{k^F_{qtct}[\mathrm{tct}]}\right) \tag{16}$$

Quantum yields in the presence of O_2 starting from *ttt*-DPH in Bz and MCH (Tables 4 and 5, respectively) are consistent with eq 14 and 15, Figure 2. The solvent dependence of the intersystem crossing yield of fluorenone ($\phi_{is} = 1.00$, 0.93 and 0.48 in MCH,[48] Bz,[23,25] and CH_3CN,[48] respectively) was taken into account in these and subsequent plots.

We consider first the results for MCH (Figure 2b) for which DPH mass balance was established by HPLC. The fourth experiment in Table 1 (footnote d) and the second row in Table 2 show that at least 97% of DPH is accounted for as one of its isomers even after a prolonged irradiation period, far exceeding irradiation times employed in quantum yield measurements.

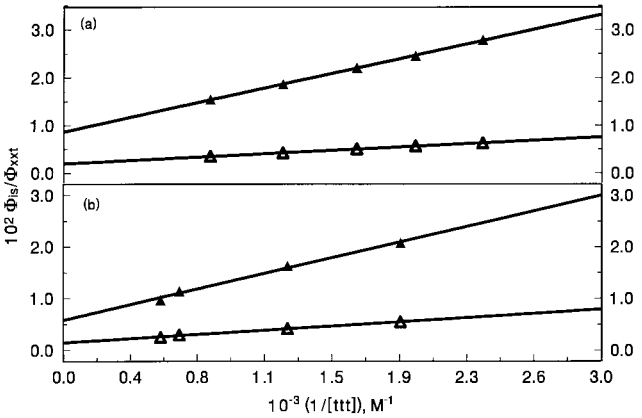

Figure 2. Plots of *tct*- (△) and *ctt*-DPH (▲) formation quantum yields for the fluorenone-sensitized photoisomerization of *ttt*-DPH in air-saturated (a) benzene and (b) methylcyclohexane, based on eqs 14 and 15.

Depletion of O_2 during the course of these experiments can, therefore, be assumed to be negligible. The intercepts in Figure 2b give $\epsilon = 0.017 \pm 0.002$ and $\zeta = 0.069 \pm 0.007$. These fractions should be close to the fractional contributions of *ctt*- and *tct*-DPH triplets, respectively, in ^{3}eet* in MCH at 20 °C. As expected on the basis of eqs 14 and 15, the two lines in Figure 2b have essentially identical intercept to slope ratios (i/s) $= k^F_{qttt}/(k^F_{qox}[O_2]) = (7.2 \pm 1.2) \times 10^2$ and $6.7 \pm 1.0 \times 10^2$ M^{-1} for *ctt*- and *tct*-DPH, respectively. These values are in excellent agreement with $k^F_{qttt}/(k^F_{qox}[O_2]) = 6.8 \times 10^2$ M^{-1} calculated on the basis of reasonable estimated values of the quenching rate constants of the fluorenone triplets, $k^F_{qttt} = 5 \times 10^9$ M^{-1} s^{-1} and $k^F_{qox} = 3 \times 10^9$ M^{-1} s^{-1},[42] and $[O_2] = 2.46 \times 10^{-3}$ M.[49] The intercepts in Figure 2a give $\epsilon = 0.0115 \pm 0.0002$ and $\zeta = 0.0500 \pm 0.0014$ in Bz at 20 °C. These fractions suggest a somewhat lower contribution of the ctt and tct triplets in the equilibrium composition in Bz than in MCH, in agreement with the trend in the photostationary fractions in Table 2. The (i/s) ratios are again in excellent agreement, giving $k^F_{qttt}/(k^F_{qox}[O_2])$ values of $(1.066 \pm 0.023) \times 10^3$ and $(1.075 \pm 0.036) \times 10^3$ M^{-1} for the ctt and tct lines, respectively. They are consistent with the expected value of 1.04×10^3 M^{-1} based on $k^F_{qtxx}/k^F_{qox} = 5/3$ and $[O_2] = 1.6 \times 10^{-3}$ M.[42] Based on eqs 14 and 15, ϕ_{is}/ϕ_{ctt} vs $[\mathrm{tct}]^{-1}$ and ϕ_{is}/ϕ_{tct} vs $[\mathrm{ctt}]^{-1}$ plots (Tables 7 and 8) are expected to have identical intercepts as the plots in Figure 2a. Intercepts of 87 ± 2 and 90 ± 6 are obtained for ctt formation starting from *ttt*- and *tct*-DPH, respectively. The corresponding values for tct formation are 20.0 ± 0.6 and 18 ± 8 starting from *ttt*- and *ctt*-DPH, respectively. In view of this very good agreement, the plots of the quantum yields in all directions starting from each of the three DPH isomers (six data sets) are forced to three common intercepts in Figure 3. The three common intercepts give $\epsilon = 0.011$, $\zeta = 0.050$, and $1 - \epsilon - \zeta = 0.938$ (Table 10). The sum of these values is almost exactly unity, although the 10% standard deviation in the $1 - \epsilon - \zeta$ value leaves something to be desired. We conclude that, within experimental uncertainty, the lifetime of DPH triplets in the presence of air, 100 ns,[16,17] is sufficient to allow their full equilibration. Since the lifetime of the DPH triplets is in the microsecond time scale in degassed solutions, the isomeric triplets must be equilibrated in the absence of O_2.

Relative rate constants for triplet excitation transfer from fluorenone to the DPH isomers can be estimated from the decay fractions for O_2 quenching (Table 10) and the photostationary state composition in Table 2 using eqs 12 and 13: $k^F_{qttt}:k^F_{qct}:$

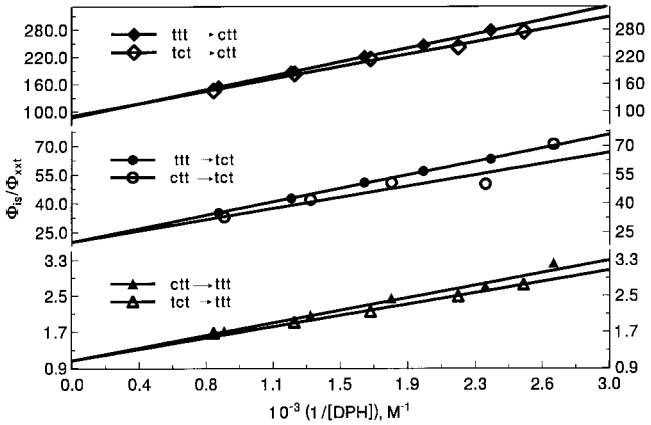

Figure 3. As in Figure 2 for air-saturated benzene solutions of *ttt*-, *tct*-, and *ctt*-DPH in the directions shown.

TABLE 10: Geometric Composition of DPH Triplets Based on Quantum Yields for Air-Saturated Benzene Solutions[a]

DPH[b]	ϵ	ζ	$1-\epsilon-\zeta$
ttt	0.0115(2)	0.0500(1)	
tct	0.0111(7)		0.88(4)
ctt		0.057(25)	0.97(11)
global[c]	0.0111(8)	0.0500(5)	0.938(97)

[a] Values in parentheses are standard deviations in last significant figures shown. [b] Starting DPH isomer. [c] From the common intercept lines in Figure 3.

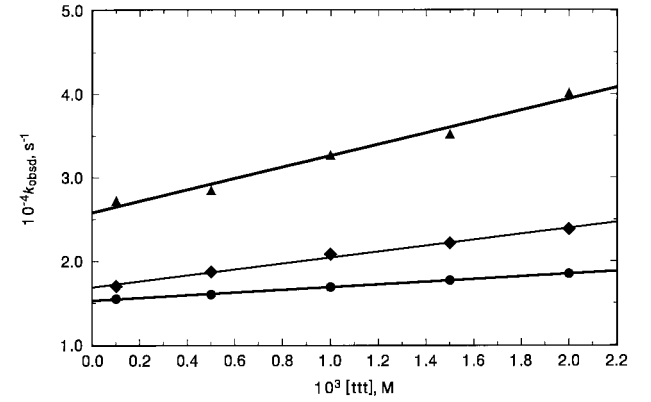

Figure 4. Dependence of observed ^{3}DPH* decay rate constants on *ttt*-DPH concentration in degassed acetonitrile (▲), benzene (◆), and methylcyclohexane (●).

$k^F_{qtct} = 1.00:1.53:1.61$. This calculation may underestimate the relative magnitude of k^F_{qttt} because it assumes no DPH loss during the irradiation time employed for the measurement of the photostationary states. However, the observed independence of the photostationary compositions in Table 2 on total [DPH] is consistent with this assumption since any fractional irreversible loss of DPH would diminish with increased [DPH]. A slightly narrower range of quenching constants is predicted if the decay fractions are based on the quantum yield ratios in Tables 4, 7, and 8 instead of on the intercepts of the global plots in Figure 4: $k^F_{qttt}:k^F_{qctt}:k^F_{qtct} = 1.00:1.35:1.51$. Differences in these excitation transfer rate constants should also be reflected in the *i*/*s* ratios of the lines in Figure 3. The $k^F_{qttt}/(k^F_{qox}[O_2]) = (1.07 \pm 0.04) \times 10^3\ M^{-1}$ is narrowly defined by the two sets of quantum yields starting from the ttt isomer. The lines corresponding to the other two isomers are less self-consistent. Assuming that the larger quantum yields for ttt formation are more accurate because they are insensitive to back reaction corrections, the *i*/*s* ratios for the common intercept lines give $k^F_{qctt}/(k^F_{qox}[O_2]) = 1.39 \times 10^3\ M^{-1}$ and $k^F_{qtct}/(k^F_{qox}[O_2]) = 1.60 \times 10^3\ M^{-1}$. This corresponds to $k^F_{qttt}:k^F_{qtct}:k^F_{qtct} = 1.00:1.30:1.49$. Since the triplet excitation energy of fluorenone is 53 kcal/mol[50] and excitation energies of the DPH isomers are in the 34−36 kcal/mol[15,31,51] range, highly exothermic excitation transfers are involved. The results reveal a small selectivity between the trienes that may reflect a higher exothermicity of the excitation transfer to the ttt isomer.

The relative free energies of the isomeric DPH triplets can be estimated from the decay fractions in Table 10, and, in the case of *cct*-DPH, from its contribution in the photostationary state in the presence of air (Table 2). With the *ttt*-DPH triplet assigned a free energy of zero, the values for the *tct*-, *ctt*-, and *cct*-DPH triplets are 1.7, 2.6, and 5.1 kcal/mol, respectively. Since entropy contributions are expected to be small, the same relative order is expected in the enthalpies and in the potential energies of the triplet states of these isomers. The identical enthalpy order obtains in the ground state.[52]

Transient Observations. The DPH triplet−triplet absorption spectra measured in this work (Figure 1) are in good agreement with earlier measurements for *ttt*-DPH.[15−17] The complete equilibration of the isomeric DPH triplets in the time scale of these measurements (21 μs) is confirmed by the observation of identical spectra starting from *ttt*-, *tct*-, or *ctt*-DPH solutions. The precautions of using a flow cell and exposing the solutions to very low energy laser pulses were essential in avoiding extensive DPH photoisomerization during the course of the measurements. Initial observations using static cells and higher energy pulses gave identical spectra to those in Figure 1, independent of the identity of the DPH isomer employed. However, these preliminary results were invalidated by HPLC analysis at the end of the spectral measurements that showed all solutions to have attained the identical photostationary state composition.

The longest triplet lifetime reported for *ttt*-DPH triplets is 400 μs in EPA (diethyl ether, isopentane, ethanol in 5:5:2 ratio by volume) glass at 77 K[31] and in 2-methyltetrahydrofuran at −150 °C.[16] Both of these media are sufficiently rigid to ensure that the DPH triplet maintain its all-trans geometry throughout its lifetime. Triplet lifetimes in the 10−100 μs range have been reported at 22 and 25 °C in fluid solutions[16,17] that do not restrict torsional motions of the molecule. Compared to stilbene triplets for which the lifetime change is more than a million-fold for analogous medium/temperature changes,[31,43,53] the change in the lifetime of DPH triplets is modest. It is consistent with a photoisomerization mechanism in which all decay is from essentially planar isomeric triplet states that are in dynamic equilibrium, and precludes significant residence times in triplets with perpendicular geometries about any of the double bonds.[16,17]

Earlier measurement of DPH triplet lifetimes in solution at ambient temperatures were made using argon-purging to exclude O_2 and laser pulses in the mJ power range.[16,17] These lifetimes are shorter than ours. Significantly longer lifetimes of 100 and 70 μs in benzene and acetonitrile, respectively, were obtained using conventional flash photolysis on dilute solutions, [*ttt*-DPH] $\leq 2 \times 10^{-5}$ M.[16] Since higher concentrations were employed in the laser experiments, the shorter triplet lifetimes were attributed to quenching of DPH triplets by ground-state DPH molecules ("self-quenching").[16] Observed first-order decay rate constants, k_{obsd}, were expressed as

$$k_{obsd} = \tau_0^{-1} + k_{sq}[DPH] \qquad (17)$$

and k_{sq} was estimated to lie in the $(1-3) \times 10^8\ M^{-1}\ s^{-1}$ range.[16]

TABLE 11: Lifetimes and Self-Quenching Rate Constants[a]

		$10^6 k_{sq}$, M^{-1} s^{-1}		
solvent	τ_0, μs	*ttt*-DPH	*tct*-DPH	*ctt*-DPH
Bz	59.3 (0.8)	3.54 (0.18)	3.69	4.27
AN	65.4 (0.2)	1.60 (0.04)		
MCH	38.7 (1.0)	6.81 (0.58)		

[a] Values in parentheses are standard deviations for the intercepts and slopes in Figure 4.

In terms of our mechanism, $\tau_0 = 1/k_d$ in eq 6, and, for *ttt*-DPH, $k_{sq} = (1 - \gamma - \delta)k_{ttt}$ in eq 7. The lifetimes in Table 9 decrease with increasing [*ttt*-DPH], adhering closely to eq 17 (Figure 4). The intercepts and slopes of the plots give the τ_0 and k_{sq} values in Table 11. While the τ_0 values are in the same ball park as the previously reported lifetimes, the k_{sq} values are 2 orders of magnitude smaller. Measurement of self-quenching rate constants is a nontrivial matter because any quenching impurity in the sample of interest would lead to a concentration dependence that can be mistaken for self-quenching.[54] Lifetimes of DPH triplets were measured for a single concentration each of *tct*- and *ctt*-DPH in benzene. Together with the τ_0 values in Table 11, they yield the quenching rate constants shown in the last two columns of Table 11. The magnitude of these rate constants is remarkably independent of the identity of the DPH isomer participating in the quenching process. This result suggests that summary eqs 7−9 in our mechanism are not strictly correct. If, for instance, in the case of *ctt*-DPH, quenching involved interaction of ^{3}ctt* with the corresponding ground state isomer, ^{1}ctt, as self-quenching is normally envisioned, then the actual rate constant for that event would have to be ~100 times larger than for the same process for *ttt*-DPH. This follows from our conclusion that ^{3}ctt* comprises roughly 1% of the DPH triplet population in benzene. It seems more likely that interactions between the dominant triplet isomer, ^{3}ttt*, with the ground states of *ctt*- and *tct*-DPH lead not only to triplet excitation transfer, as shown in eqs 8 and 9, but also to quenching. Such competitions can be accommodated by our mechanism by splitting the γ and δ fractions in eqs 7−9 into energy transfer (γ_{en} and δ_{en}) and quenching (γ_q and δ_q) parts. For instance, eq 7 can be written as

$$^3\text{eet}^* + {}^1\text{ttt} \xrightarrow{k_{ttt}} \gamma\,{}^1\text{ctt} + \delta\,{}^1\text{tct} + (\gamma_{en} + \delta_{en})\,{}^3\text{eet}^* + [2(1 - \gamma - \delta) + \gamma_q + \delta_q]\,{}^1\text{ttt} \quad (18)$$

where $\gamma = \gamma_{en} + \gamma_q$ and $\delta = \delta_{en} + \delta_q$, and analogous changes can be made in eqs 8 and 9.

Photochemistry in Degassed Solutions. Starting from *ttt*-DPH, ϕ_{ctt}/ϕ_{tct} ratios show a modest dependence on solvent. They range from 0.17 ± 0.01 in CH_3CN to 0.51 ± 0.02 in CCl_4 (Table 6), with hydrocarbon solvents MCH and Bz having a nearly identical intermediate value of 0.24 ± 0.01 (Tables 4 and 5). Since in the latter two solvents the ratio can be seen to be unaffected by the presence of O_2, it is tempting to conclude that the quantum yield ratios reveal the solvent dependence of the [^{3}ctt*]/[^{3}tct*] ratio of the equilibrated triplets. Although photoisomerization quantum yields are 10−20 times larger when O_2 is removed from the DPH solutions, their ratios are independent of [O_2] and of [DPH]. Based on our mechanism, quantum yield ratios starting from *ttt*-DPH are given by

$$\frac{\phi_{ctt}}{\phi_{tct}} = \frac{\alpha + \gamma k_{ttt}\tau_0[^1\text{ttt}]}{\beta + \delta k_{ttt}\tau_0[^1\text{ttt}]} \quad (19)$$

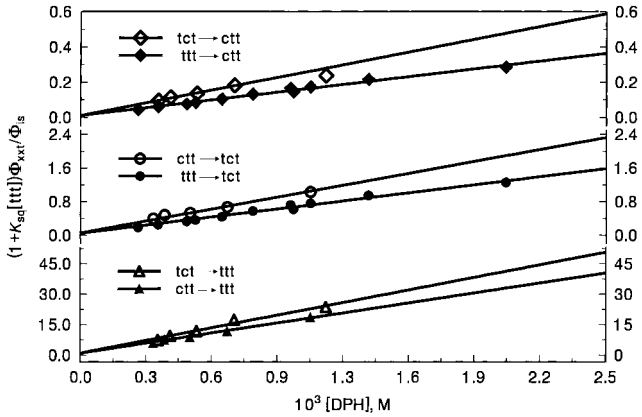

Figure 5. Plots of photoisomerization quantum yields of the DPH isomers in degassed benzene solutions in the directions shown based on eqs 22 and 23 for *ttt*-DPH and analogous eqs for *tct*- and *ctt*-DPH.

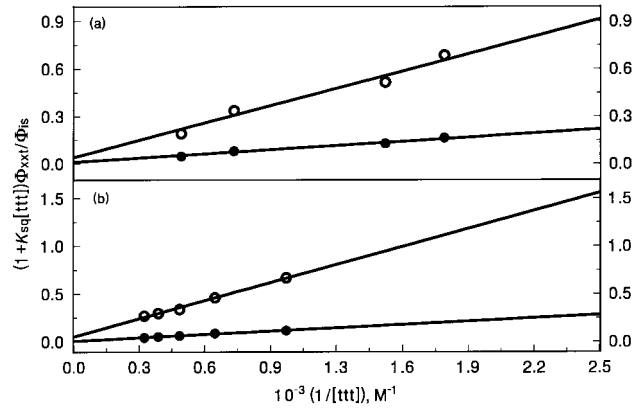

Figure 6. As in Figure 5 starting from *ttt*-DPH in degassed (a) methylcyclohexane and (b) acetonitrile; ϕ_{tct} (○), ϕ_{ctt} (●).

and analogous expressions can be written for the other directions. The [DPH] independence of these ratios can be accounted for either if α and β are small compared to the second terms in the numerator and denominator, respectively, or if $(\alpha/\beta) = (\gamma/\delta)$. Either of these conditions reduces the right-hand side of eq 19 to γ/δ.

Quantum yields starting from *ttt*-DPH are given by

$$\frac{\phi_{ctt}}{\phi_{is}} = \frac{\alpha + \gamma k_{ttt}\tau_0[^1\text{ttt}]}{1 + (1 - \gamma_{en} - \delta_{en})k_{ttt}\tau_0[^1\text{ttt}]} \quad (20)$$

$$\frac{\phi_{tct}}{\phi_{is}} = \frac{\beta + \delta k_{ttt}\tau_0[^1\text{ttt}]}{1 + (1 - \gamma_{en} - \delta_{en})k_{ttt}\tau_0[^1\text{ttt}]} \quad (21)$$

Since $k_{sq} = (1 - \gamma_{en} - \delta_{en})k_{ttt}$, the common denominators in eqs 20 and 21 are known in all solvents except CCl_4 (Table 11). Rearrangement of eqs 20 and 21 gives

$$(\phi_{ctt}/\phi_{is})(1 + K_{sq}[^1\text{ttt}]) = \alpha + \gamma k_{ttt}\tau_0[^1\text{ttt}] \quad (22)$$

$$(\phi_{tct}/\phi_{is})(1 + K_{sq}[^1\text{ttt}]) = \beta + \delta k_{ttt}\tau_0[^1\text{ttt}] \quad (23)$$

where $K_{sq} = k_{sq}\tau_0$. The quantum yields in Bz, MCH, and AN are plotted according to eqs 22 and 23 in Figures 5 and 6. The intercepts of these plots are within experimental error of zero. This is because the observed quantum yields are much larger than quantum yields expected from the unimolecular decay of the equilibrated triplets. The data are not sufficiently precise

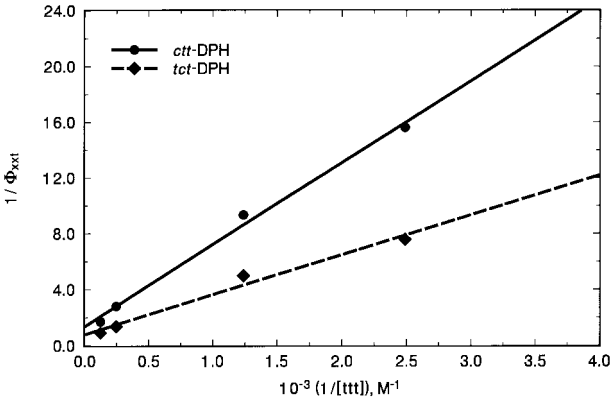

Figure 7. Quantum yields for the fluorenone-sensitized photoisomerization of *ttt*-DPH in degassed carbon tetrachloride plotted according to eqs 24 and 25.

to define α and β, the unimolecular contributions to the photoisomerization, because the quantum chain processes are the dominant photoisomerization pathways in all directions. Assuming that the decay rate constants of the isomeric DPH triplets do not differ significantly in magnitude, α and β should be roughly equal to ϵ and ζ, respectively. The latter are known in benzene (Table 10) and were used to fix the intercepts of the plots in Figure 5. In the case of methylcyclohexane the uncertainties in ϵ and ζ values from Figure 2b are large and the photostationary state in the presence of air (Table 2) was used instead to estimate ϵ and ζ values (Figure 6a). In the case of acetonitrile the intercepts were not fixed (Figure 6b).

Since neither lifetime nor ϵ and ζ measurements were made in CCl_4, the photoisomerization yields in this solvent could not be treated as fully. By assuming that α and β are negligible relative to the quantum chain terms, rearrangement of eqs 20 and 21 gives

$$\frac{\phi_{is}}{\phi_{ctt}} = \frac{(1-\gamma_{en}-\delta_{en})}{\gamma} + \frac{1}{\gamma k_{ttt}\tau_0[^1ttt]} \qquad (24)$$

$$\frac{\phi_{is}}{\phi_{tct}} = \frac{(1-\gamma_{en}-\delta_{en})}{\delta} + \frac{1}{\delta k_{ttt}\tau_0[^1ttt]} \qquad (25)$$

The quantum yields for the photoisomerization of *ttt*-DPH in CCl_4 (Table 6) are plotted according to eqs 25 and 26 in Figure 7. Based on these equations, the two lines in Figure 7 should have identical $i/s = k_{sq}\tau_0$. Our results, $k_{sq}\tau_0 = (2.3 \pm 0.8) \times 10^2$ and $(2.7 \pm 1.4) \times 10^2$ M^{-1} for ϕ_{ctt} and ϕ_{tct}, respectively, are in reasonable agreement with this expectation. Furthermore, the magnitude of $k_{sq}\tau_0$ is consistent with our measurements of this quantity in the other three solvents.

Intercepts and slopes for Figures 5 and 6 are summarized in Table 12. As described in footnote *d* in this table the symbols used to designate the slopes in Figures 5 and 6 are such that, for instance, $s_{01} = \gamma k_{ttt}\tau_0$ and $s_{30} = \delta'' k_{tct}\tau_0$. Since, as will be shown below, the rate constants for the triplet excitation transfer steps among the DPH isomers are about 2 orders of magnitude larger than the self-quenching rate constants, γ_q and δ_q contributions to γ and δ in eqs 7−9 can be neglected. The τ_0 values in Table 11 were employed to convert the slopes in Table 12 to effective rate constants, e.g., γk_{ttt} and $\delta'' k_{tct}$ from slopes s_{01} and s_{30}, respectively. The fractional populations of the isomeric quenched triplets must be taken into account in order to convert these quantities to rate constants for molecular events. Neglecting the trace presence of ^{3}cct*, the equilibrium fractions of the major isomeric triplets are given by

TABLE 12: Quantum Chain Parameters[a]

DPH[b]	α	β	$1-\alpha-\beta$	$10^{-2}s_{i0}$, M^{-1}	$10^{-2}s_{i1}$, M^{-1}	$10^{-2}s_{i3}$, M^{-1}
			Bz			
ttt	0.011(1)	0.050(3)			1.41(5)	6.13(25)
tct	0.011(1)		0.94(80)	199(12)	2.31(5)	
ctt		0.055(5)	0.94(40)	158(7)		9.07(54)
			MCH			
ttt	0.011(6)	0.041(30)			0.83(5)	3.49(27)
			AN[b]			
ttt	0.007(5)	0.052(16)			1.10(7)	6.03(25)

[a] Values in parentheses are standard deviations for the fixed intercept plots; s_{ij} are the slopes in Figures 5-7, where *i* and *j* designate the starting DPH isomer and the product isomer, respectively, with 0, 1, and 3 indicating *ttt*-, *ctt*-, and *tct*-DPH, respectively. [b] Intercepts were not fixed in this case.

TABLE 13: Rate Constants for Triplet Excitation Transfer between DPH Isomers

acceptor	$10^{-8}k_{i0}$*, M^{-1} s^{-1}	$10^{-8}k_{i1}$*, M^{-1} s^{-1}	$10^{-8}k_{i3}$*, M^{-1} s^{-1}
		Bz[a]	
^{1}ttt		2.0_9	2.0_7
^{1}ctt	2.8_4		3.0_6
^{1}tct	3.5_8	3.5_1	
		MCH[b]	
^{1}ttt		2.0	2.2
		AN[c]	
^{1}ttt		1.7	1.8

[a] Based on ϵ and ζ values in Table 10, see text. [b] Based on $\epsilon = 0.011$ and $\zeta = 0.041$, Table 2. [c] Based on assumed values of $\epsilon = 0.010$ and $\zeta = 0.050$.

$$^3f_{ttt}^* = \frac{1}{1+K_{01}+K_{03}} \qquad (26)$$

$$^3f_{tct}^* = \frac{K_{03}}{1+K_{01}+K_{03}} \qquad (27)$$

$$^3f_{ctt}^* = \frac{K_{01}}{1+K_{01}+K_{03}} \qquad (28)$$

where the equilibrium constants are defined in eq 11. These fractions are equal to $1-\epsilon-\zeta$, ζ, and ϵ, respectively, and are reported for benzene in Table 10. Division of each effective rate constant by the appropriate fraction gives the excitation transfer rate constants, k_{ij}^*, where *i* is the acceptor DPH isomer and *j* is the donor triplet, listed in Table 13.

Excitation Transfer Steps in the Quantum Chain Processes. The rate constants in Table 13 are all, roughly, an order of magnitude smaller than the value expected for a diffusion-controlled reaction. They are very close to $k_{en} = 2.6 \times 10^8$ M^{-1} s^{-1}, the rate constant for the propagation step of the triplet quantum chain process in the photoisomerization of *cis*-1-(2-anthryl)-2-phenylethene, *c*-APE.[36,39,40,55]

$$^3t\text{-APE}^* + {}^1c\text{-APE} \xrightarrow{k_{en}} {}^1t\text{-APE} + {}^3c\text{-APE}^* \qquad (29)$$

The remarkable similarity in the magnitude of the rate constants and the lack of selectivity in the function of each ground state DPH isomer as an acceptor of triplet excitation from the other two isomers accounts for the near identity of ϵ/ζ and γ/δ ratios.

Ratios of the rate constants in Table 13 predict the equilibrium constants for triplet excitation transfer between DPH isomers,

$$^3\text{ctt}^* + {}^1\text{ttt} \overset{K_{01}^*}{\rightleftharpoons} {}^3\text{ttt}^* + {}^1\text{ctt} \quad (30)$$

$$^3\text{tct}^* + {}^1\text{ttt} \overset{K_{03}^*}{\rightleftharpoons} {}^3\text{ttt}^* + {}^1\text{tct} \quad (31)$$

$$^3\text{tct}^* + {}^1\text{ctt} \overset{K_{13}^*}{\rightleftharpoons} {}^3\text{ctt}^* + {}^1\text{tct} \quad (32)$$

$K_{01}^* = k_{01}^*/k_{10}^* = 0.74$, $K_{03}^* = k_{03}^*/k_{03}^* = 0.58$, and $K_{13}^* = k_{13}^*/k_{31}^* = 0.87$ in eqs 30, 31, and 32, respectively. The K_{03}^*/K_{01}^* ratio gives $K_{13}^* = 0.79$, well within experimental uncertainty of 0.87, demonstrating the self-consistency of the rate constants. The equilibrium constants correspond to free energy differences of 0.18, 0.32, and 0.08 kcal/mol for eqs 30, 31, and 32, respectively. Although the excitation transfer events depicted in these equations are nearly free energy neutral, since the temperature dependence of the K_{ij}^*'s is not known, the possibility must be considered that this result is due to compensating enthalpy and entropy changes. Examples of reversible intermolecular triplet excitation transfer were first published in 1964,[56,57] and studies of the temperature dependence of equilibrium constants for such processes appeared more than 20 years later.[58,59] As expected, ΔS is nearly zero when donor and acceptor molecules have rigid structures that allow little, if any, change in conformational freedom upon undergoing S_0-T_1 transitions.[58,59] Close correspondence in the equilibrium geometries of the final and initial states of donor and acceptor ensure that vertical coupled transitions are involved in the two partners. Nonzero ΔS values, in the range of -2 to $+4$ gibbs/mol, were obtained when one or both of the partners is a flexible molecule that undergoes change in equilibrium geometry and conformational freedom on passing from one state to the other. Although the DPH isomers can be regarded as flexible molecules with considerable torsional freedom about essential single bonds, it is unlikely that their S_0-T_1 transitions involve significant entropy changes. The reversal of single/double bond character in the triene moiety that accompanies such transitions simply transfers the relative ease of torsional motion to different bonds. Therefore, we infer from the small ΔG's that the corresponding ΔH's are also small and that, accordingly, the triplet excitation energies of the DPH isomers cannot differ by more than 1 or 2 kcal/mol. *At the planar geometries the triplet potential energy surface of DPH very nearly parallels the ground state energy surface*.

Exothermic triplet excitation transfer involving $\pi-\pi^*$ transitions between rigid aromatic hydrocarbons is almost diffusion controlled.[42] For instance, the rate constant for triplet excitation transfer from indeno[2,1-*a*]indene to azulene is 8.9×10^9 M^{-1} s^{-1} at 298 °C in toluene.[60] Sandros reasoned that when donor and acceptor triplet energies are identical, reversible excitation transfer between the two partners would be faster than diffusional separation of the encounter complex, such that the rate constant in either direction should drop to one-half the maximum value.[56] The rate constants in Table 13 are 25−40 times smaller than this limit, notwithstanding ΔE_T's that must be close to zero. We suggest that, although essentially planar equilibrium geometries are involved in the S_0 and T_1 states of both donor and acceptor, substantial differences in these geometries render triplet excitation transfer between DPH isomers nonvertical.[61−66] Unfavorable Franck−Condon overlap factors, involving primarily stretching and torsional vibrations of the triene moiety, would then account for the inefficiency of the excitation transfer steps.

Conclusion

Earlier quantum chain photoisomerization mechanisms for conjugated alkadienes,[34] alkatrienes,[35] and 1,4-diphenyl-1,3-butadienes[37] were based on triplets with twisted equilibrium geometries (one of the ground state double bonds twisted to ~90°) as the chain carrying species. How such nonplanar triplets gave the S_0 state of the product polyene upon transferring excitation to an isomeric polyene was left rather vague. In the initial demonstration of this process for the 1,3-pentadienes and the 2,4-hexadienes, it was recognized that the occurrence of such excitation transfer steps places a limit on the energy differences between planar and twisted triplets.[34] For DPH, we have now presented strong evidence implicating equilibrated isomeric planar triplets as the quantum chain carriers. It is tempting to speculate that the chain carriers in the earlier systems are similarly planar triplets present in equilibrium with the usually dominant twisted triplets. It is likely that the quantum chain mechanism for the 1,4-diphenyl-1,3-butadienes, whose triplet lifetime (1.6 μs)[17,37] most closely approaches that of DPH, resembles that of DPH.

Acknowledgment. This research was supported by NSF, most recently, by Grant CHE-9612316. The use of the Chemistry Departmental Laser Laboratory facilities is gratefully acknowledged.

References and Notes

(1) Hudson, B. S.; Kohler, B. E. *Annu. Rev. Phys. Chem.* **1974**, *25*, 437−460.
(2) Hudson, B. S.; Kohler, B. E.; Schulten, K. In *Excited States*; Lim, E. C., Ed.; Academic Press: New York, 1982; Vol. 6, pp 1−95.
(3) Saltiel, J.; Sun, Y.-P. In *Photochromism, Molecules and Systems*; Dürr, H.; Bouas-Laurent, H., Eds.; Elsevier: Amsterdam, 1990; pp 64−164.
(4) Orlandi, G.; Siebrand, W. *Chem. Phys. Lett.* **1975**, *30*, 352−354.
(5) Itoh, T.; Kohler, B. E. *J. Phys. Chem.* **1987**, *91*, 1760−1764.
(6) Hilinski, E. F.; McGowan, W. M.; Sears, D. F., Jr.; Saltiel, J. *J. Phys. Chem.* **1996**, *100*, 3308−3311.
(7) Saltiel, J.; Ko, D.-H.; Fleming, A. S. *J. Am. Chem. Soc.* **1994**, *116*, 4099−5000.
(8) Saltiel, J.; Wang, S. *J. Am. Chem. Soc.* **1995**, *117*, 10761−10762.
(9) (a) Allen, M. T.; Whitten, D. G. *Chem. Rev.* **1989**, *89*, 1691−1702. (b) Whitten, D. G. *Acc. Chem. Res* **1993**, *26*, 502−509.
(10) Waldeck, D. H. *Chem. Rev.* **1991**, *91*, 415−436.
(11) Kohler, B. E. *Chem. Rev.* **1993**, *93*, 41−54.
(12) (a) Birks, J. B.; Birch, D. J. S. *Chem. Phys. Lett.* **1975**, *31*, 608−610. (b) Birks, J. B.; Tripathi, G. N. R.; Lumb, M. D. *Chem. Phys.* **1978**, *33*, 185−194. (c) Birks, J. B. *Chem. Phys. Lett.* **1978**, *54*, 430−434.
(13) Goldbeck, R. A.; Twarowski, A. J.; Russell, E. L.; Rice, J. K.; Birge, R. R.; Switkes; E.; Kliger, D. S. *J. Chem. Phys.* **1982**, *77*, 3319−3328.
(14) Chattopadhyay, S. K.; Das, P. K. *Chem. Phys. Lett.* **1982**, *87*, 145−150.
(15) Bensasson, R.; Land, E. J.; Lafferty, J.; Sinclair, R. S.; Truscott, T. G. *Chem. Phys. Lett.* **1976**, *41*, 333−335.
(16) Görner, H. *J. Photochem.* **1982**, *19*, 343−356.
(17) Chattopadhyay, S. K.; Das, P. K.; Hug, G. L. *J. Am. Chem. Soc.* **1982**, *104*, 4507−4514.
(18) Values in ref 15 have been adjusted upward because a low value was employed for ϕ_{is} of the anthracene standard.[19]
(19) Wilkinson, F. In *Organic Molecular Photophysics*; Birks, J. B., Eds.; Wiley: London, 1975; pp 95−158.
(20) Saltiel, J.; Sears, D. F., Jr.; Ko, D.-H.; Park, K. M. In *Handbook of Organic Photochemistry and Photobiology*; Horspool, W. M., Song, P.-O., Eds.; CRC Press: London, 1995; Section 1, pp 3−15.
(21) Saltiel, J. *J. Am. Chem. Soc.* **1968**, *90*, 6394−6400.
(22) Saltiel, J.; Townsend, D. E.; Watson, B. D.; Shannon, P.; Finson, S. *J. Am. Chem. Soc.* **1977**, *99*, 884−896.
(23) Caldwell, R. A.; Gajewski, R. P. *J. Am. Chem. Soc.* **1971**, *93*, 532−534.
(24) Valentine, D., Jr.; Hammond, G. S. *J. Am. Chem. Soc.* **1972**, *94*, 3449−3454.
(25) Lamola, A. A.; Hammond, G. S. *J. Chem. Phys.* **1965**, *43*, 2129−2135.

(26) Saltiel, J.; Marinari, A.; Chang, D. W.-L.; Mitchener, J. C.; Megarity, E. D. *J. Am. Chem. Soc.* **1979**, *101*, 2982−2996.
(27) Wagner, P. J. In *Creation and Detection of the Excited State*; Lamola, A. A., Ed.; Marcel Dekker: New York, 1971; Vol. 1, Part A.
(28) Ko, D.-H. Ph.D. Dissertation, The Florida State University, Tallahassee, FL 1997.
(29) Lunde, K.; Zechmeister, L. *J. Am. Chem. Soc.* **1954**, *76*, 2308−2313.
(30) Unett, D. J.; Caldwell, R. A. *Res. Chem. Intermed.* **1995**, *21*, 665−709.
(31) Heinrich, G.; Holzer, G.; Blume, H.; Schulte-Frohlinde, D. *Z. Naturforsch.* **1970**, *25B*, 496−499.
(32) Wu, K. C.; Trozzolo, A. M. *J. Phys. Chem.* **1979**, *83*, 3180−3183.
(33) Chattopadhyay, S. K.; Kumar, C. V.; Das, P. K. *J. Phys. Chem.* **1985**, *89*, 670−673.
(34) Saltiel, J.; Townsend, D. E.; Sykes, A. *J. Am. Chem. Soc.* **1973**, *95*, 5968−5973.
(35) Butt, Y. C. C.; Singh, A. K.; Baretz, B. H.; Liu, R. S. H. *J. Phys. Chem.* **1981**, *85*, 2091−2097.
(36) Arai, T.; Karatsu, T.; Misawa, H.; Kuriyama, Y.; Okamoto, H.; Hiresake, T.; Furuuchi, H.; Zeng, H.; Sakuragi, H.; Tokumaru, K. *Pure Appl. Chem.* **1988**, *60*, 989−998 and references cited.
(37) Yee, W. A.; Hug, S. J.; Kliger, D. S. *J. Am. Chem. Soc.* **1988**, *110*, 2164−2169.
(38) Ganapathy, S.; Liu, R. S. H. *J. Am. Chem. Soc.* **1992**, *114*, 3459−3464.
(39) Arai, T.; Tokumaru, K. *Chem. Rev.* **1993**, *93*, 23−39.
(40) Tokumaru, K.; Arai, T. *Bull. Chem. Soc. Jpn* **1995**, *68*, 1065−1087.
(41) Saltiel, J.; Thomas, B. *Chem. Phys. Lett.* **1976**, *37*, 147−148.
(42) Saltiel, J.; Atwater, B. W. *Adv. Photochem.* **1988**, *14*, 1−90.
(43) Görner, H.; Schulte-Frohlinde, D. *J. Phys. Chem.* **1981**, *85*, 1835−1841.
(44) Garner, A.; Wilkinson, F. In *Singlet Oxygen*; Randy, B., Rabek, J. F., Eds.; Wiley: New York, 1978, 48−53.
(45) Gorman, A. A.; Rodgers, M. A. *J. Chem. Phys. Lett.* **1985**, *120*, 58−62.
(46) Stevens, B.; Algar, B. E. *Ann. N.Y. Acad. Sci.* **1970**, *171*, 50−60.
(47) Patterson, L. K.; Porter, G.; Top, M. R. *Chem. Phys. Lett.* **1970**, *7*, 612−614.
(48) Andrews, L. J.; Deroulede, A.; Linschitz, H. *J. Phys. Chem.* **1978**, *82*, 2304−2309.
(49) *Solubility Data Series, Oxygen and Ozone*; Battino, R., Ed.; IUPAC Commission on Solubility Data; Pergamon Press: New York, 1981; Vol. 7, pp 244 and 250 for MCH and Bz, respectively.
(50) Herkstroeter, W. G.; Lamola, A. A.; Hammond, G. S. *J. Am. Chem. Soc.* **1964**, *86*, 4537−4540. Cf., however: Yoshihara, K.; Kearns, D. R. *J. Chem. Phys.* **1966**, *45*, 1991−1999, where a value of 50 kcal/mol is given.
(51) Ramamurthy, V.; Caspar, J. V.; Corbin, D. R.; Schlyer, B. D.; Maki, A. H. *J. Phys. Chem.* **1990**, *94*, 3391−3393.
(52) Saltiel, J.; Mast, J. M.; Shujun, W. Unpublished observations.
(53) Saltiel, J.; D′Agostino, J. T.; Herkstroeter, W. G.; Saint-Ruf, G.; Buu-Hoï, N. P. *J. Am. Chem. Soc.* **1973**, *95*, 2543−2549.
(54) Saltiel, J.; Marchand, G. R.; Dabestani, R.; Pecha, J. M. *Chem. Phys. Lett.* **1983**, *100*, 219−222 and references cited.
(55) Saltiel, J.; Zhang, Y.; Sears, D. F., Jr. *J. Am. Chem. Soc.* **1997**, *119*, 11202−11210.
(56) Sandros, K. *Acta Chem. Scand.* **1964**, *18*, 2355-
(57) Hammond, G. S.; Saltiel, J.; Lamola, A. A.; Turro, N. J.; Bradshaw, J. S.; Cowan, D. O.; Counsell, R. C.; Vogt, V.; Dalton, C. *J. Am. Chem. Soc.* **1964**, *86*, 3197−3217.
(58) Scaiano, J. C.; Gessner, F. *J. Am. Chem. Soc.* **1985**, *107*, 7206−7207.
(59) Zhang, D. Closs, G. L.; Chung, D. D.; Norris, J. R. *J. Am. Chem. Soc.* **1993**, *115*, 3670−3673.
(60) Saltiel, J.; Shannon, P. T.; Zafiriou, O. C.; Uriarte, A. K. *J. Am. Chem. Soc.* **1980**, *102*, 6799−6808.
(61) Hammond, G. S.; Saltiel, J. *J. Am. Chem. Soc.* **1963**, *85*, 2516−2517.
(62) Saltiel, J.; Marchand, G. R.; Kirkor-Kaminska, E.; Smothers, W. K.; Mueller, W. B.; Charlton, J. L. *J. Am. Chem. Soc.* **1984**, *106*, 3144−3151.
(63) Gorman, A. A. *The Spectrum* **1990**, *3*, 16−20.
(64) Gorman, A. A.; Beddoes, R.; Hamblett, I.; McNeeney, S. P.; Prescott, A. L.; Unett, D. J. *J. Chem. Soc., Chem. Commun.* **1991**, 963−964.
(65) Caldwell, R. A.; Riley, S. J.; Gorman, A. A.; McNeeney, S. P.; Unett, D. J. *J. Am. Chem. Soc.* **1992**, *114*, 4424−4426.
(66) Gorman, A. A.; Hamblett, I.; Rushton, F. A. P.; Unett, D. J. *J. Chem. Soc., Chem. Commun.* **1993**, 983−984.